IEEE Access
Multidisciplinary | Rapid Review | Open Access Journal

Received February 13, 2019, accepted April 24, 2019, date of publication May 27, 2019, date of current version June 12, 2019.

Digital Object Identifier 10.1109/ACCESS.2019.2919286

Methods to Characterize the Real-World Use of Rollators Using Inertial Sensors– A Feasibility Study

MINGXU SUN[1,2], JAMES AMOR[3], CHRISTOPHER J. JAMES[3], (Senior Member, IEEE), ELEONORA COSTAMAGNA[2], SIBYLLE THIES[2], ULRICH LINDEMANN[4], JOCHEN KLENK[4,5,6], AND LAURENCE KENNEY[2]

[1]School of Electrical Engineering, University of Jinan, Jinan 250022, China
[2]Centre for Health Sciences Research, University of Salford, Salford M5 4WT, U.K.
[3]Warwick Engineering in Biomedicine, School of Engineering, University of Warwick, Warwick CV4 7AL, U.K.
[4]Department of Geriatrics and Clinic for Geriatric Rehabilitation, Robert-Bosch-Hospital, 70376 Stuttgart, Germany
[5]Institute of Epidemiology and Medical Biometry, Ulm University, 89081 Ulm, Germany
[6]Study Center, IB University of Applied Sciences Berlin, 70178 Stuttgart, Germany

Corresponding author: Laurence Kenney (l.p.j.kenney@salford.ac.uk)

This work was supported by the Engineering and Physical Sciences Research Council, Swindon, U.K., under Grant EP/M025543/1.

ABSTRACT Rollators are widely used by people with mobility problems, but previous studies have been limited to self-report approaches when evaluating their real-world effectiveness. To support studies based on more robust datasets, a method to estimate mobility parameters, such as gait speed and distance traveled, in the real world is needed. Body-worn sensors offer one approach to the problem, but rollator-mounted sensors have some practical advantages providing direct insight into patterns of walking device used, an under-researched area. We present a novel method to estimate speed and distance traveled from a single rollator-mounted IMU. The method was developed using data collected from ten rollator users performing a series of walking tasks including obstacle negotiation. The IMU data is first pre-processed to account for noise, orientation offset, and rotation-induced accelerations. The method then uses a two-stage approach. First, activity classification is used to separate the rollator data into one of three classes (movement, turning, or other). Subsequently, the speed of movement and distance traveled is estimated, using a separate estimation model for each of the three classes. The results showed high classification accuracy (precision, recall, and F1 statistics all >0.9). Speed estimation showed mean absolute errors below 0.2 m/s. Estimates for distance traveled showed errors which ranged from 5% (straight line walking) to over 70%. The results showed some promise but further work with a larger data set is needed to confirm the performance of our approach.

INDEX TERMS Activity classification, inertial sensors, machine learning, rollator, speed estimation, distance estimation.

I. INTRODUCTION

An estimated 19 million people in the US and over 6 million people in the UK live with, often age-related, reduced mobility [1], [2]. Many of the people living with reduced mobility use walking aids to assist moving around their environment. Indeed, a study carried out in five European countries concluded that walking aids were reported to be used by 29-49% of older people [3]. In the United States, approximately 4.3 million people over 65 use at least one walking aid [4], with a view to safely increasing mobility [5], and the majority of walking aid users reported using theirs on a daily basis [5], [6]. However, despite their widespread use, studies of mobility in the older people have often ignored the role played by walking aids [7], [8]. Further, almost all the studies of walking aid use outside the lab/clinic environment rely on self-report methods of data collection.

One commonly used and apparently well-accepted walking aid is the rollator [5], [6]. Brandt *et al*. reported [5] that rollator users in Denmark expressed 94% overall satisfaction with their device, 4 months after its prescription. However, rollator users have also reported challenges associated with

The associate editor coordinating the review of this manuscript and approving it for publication was Dian Tjondronegoro.

outdoor use. In a recent study [9] in which 60 four-wheeled-rollator users were interviewed, it was shown that users reported problems when walking downhill and uphill, during obstacle crossing and when walking over uneven ground. In addition, use of rollators may not necessarily help the rollator users to complete complex walking tasks, for example, opening a door against the walking direction [9]. A subsequent laboratory study showed that the quality of walking was improved when using a rollator compared to walking unaided, but the quality of walking with rollator was reduced during uphill and downhill walking compared to level walking. Body-mounted IMUs were used in this study to derive gait-metrics, including speed, stride length and cadence [10].

In clinical or laboratory setting, tests of walking speed and distance travelled over a fixed time are promising measures for evaluation and monitoring of reduced walking capacity and/or frailty [11], [12] and have traditionally been used as a metric of the value of walking aids to older people [13]. However, walking speed has not been widely captured in the real-world environment, where users face the most challenges to their mobility, but also where a minimum walking speed is essential to achieve certain activities (such as crossing the road at controlled crossings). Further, distance travelled is a widely used measure of general mobility [7], [8] and being able to capture these data without needing to instrument the user themselves with monitoring devices has merit, at least in those persons who cannot walk without the rollator. Finally, a better understanding of how walking users negotiate obstacles in the real world is important for urban designers and for those interested in falls research.

In our previous work [14], we reported a pilot study carried out in a simulated urban environment, showing promising predictions of both distance travelled and rollator velocity from data collected from a single inertial sensor unit located on the rollator. However, there were only two participants in the previous study (one healthy participant and one participant with multiple sclerosis) and this meant that further work was needed to validate our approach. Specifically, the pushing patterns observed in both participants, which were characterized by regular push events separated by still/low velocity periods, were particularly amenable to a simple approach using integration to derive velocity and distance travelled. It was unclear whether or not this pattern would also be seen in a larger sample. In addition, the testing in our previous study focused largely on steady walking bouts over a range of different surfaces, whereas urban walking is typified by challenges which interrupt steady walking, including negotiating of curbs and going through doors.

Therefore, the motivation of this paper is to develop a more robust and more generalisable approach to the characterisation of rollator use, based on rollator-mounted inertial sensor data. In this paper, we report on the development and implementation of a method to characterize rollator use using inertial sensors during both steady walking and when negotiating real-world relevant obstacles.

The novelty of this work lies in the demonstration of a robust approach to characterising rollator use by older adults, based on a simple sensor set, which could be deployed in the real world. The algorithm is developed and tested with older rollator users moving through a simulated real-world environment.

II. METHODS

A. PARTICIPANTS

Ten participants were recruited from the Robert-Bosch-Hospital in Stuttgart, Germany and experiments were carried out in the gait lab of the same hospital. The inclusion criteria were: 1) age 65 years or older, 2) able to walk household distances with a rollator, but not able to walk such distances unaided. People were excluded from the study if they showed 1) a history of head injury or concussion, 2) visual disorders not correctable by glasses, 3) diagnosed peripheral or central nerve dysfunction, 4) terminal disease, 5) or an inability to follow verbal instructions.

Participants (8 females) had a median age of 84 years (minimum = 77, maximum = 91 years), a median height of 154 cm (minimum = 152, maximum = 168 cm), and a median weight of 65.5 kg (minimum = 47, maximum = 80 kg). Experience in using a rollator varied from a few days to over 6 months. Written informed consent was obtained from all participants, and the experimental protocol was approved by the University of Tuebingen Medical Faculty Ethics committee (678/2016BO1) and the University of Salford Ethics Committee (HSCR13-48).

B. ROLLATOR AND DATA ACQUISITION SYSTEM

One IMU (Xsens MTw2 Awinda (Xsens Technologies BV, NL)) was attached to the front of the rollator (Coopers 10907C, Sunrise Medical Limited), as shown in Figure 1(C). The Mtw2 contains a 3 axis accelerometer, 3 axis rate gyroscope and magnetic field sensor and was set to sample at a frequency of 100 Hz. The full scale ranges for the accelerometer and rate gyroscope sensors are ± 160 m/s^2 and ± 2000 deg/s. To obtain the ground truth, the three-dimensional coordinate data of the rollator were captured from three clusters of markers using an eight-camera VICON Motion Capture System (Vicon Motion Systems Ltd, Los Angeles, USA) at a sampling frequency of 200 Hz, as shown in Figure 1(B).[1]

C. EXPERIMENTAL PROCEDURE

Each participant pushed the rollator along a pre-defined designated route, involving six activities (Figure 2): straight line walk (5 m); 90° turn; 180° turn; obstacle crossing (involving pushing two wheels of the rollator over the end part of a long wooden beam, cross section 22 mm high and 62 mm wide, while the other two wheels remain on the level floor); forward-backwards walk (2.5 m) as if to open a door;

[1] Multiple clusters were used to reduce occlusion issues

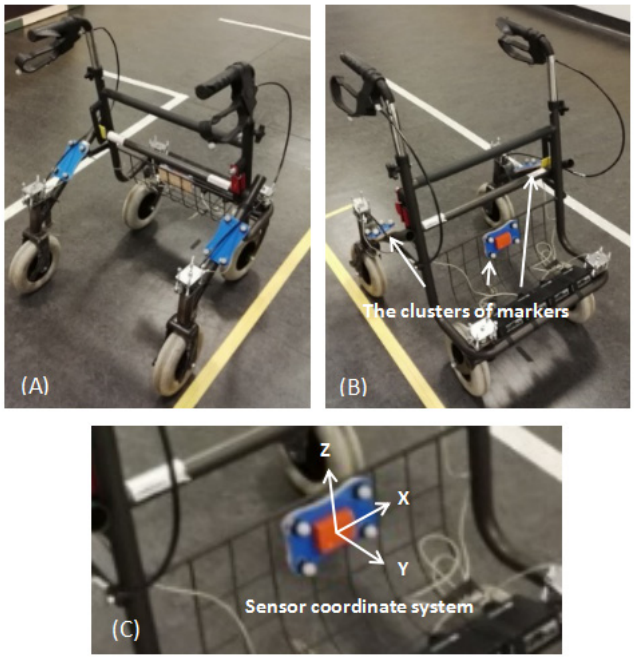

FIGURE 1. Photographs of the rollator and IMU used during the experiments showing A. rear view; B. front view; and C. accelerometer mounting with axis orientation.

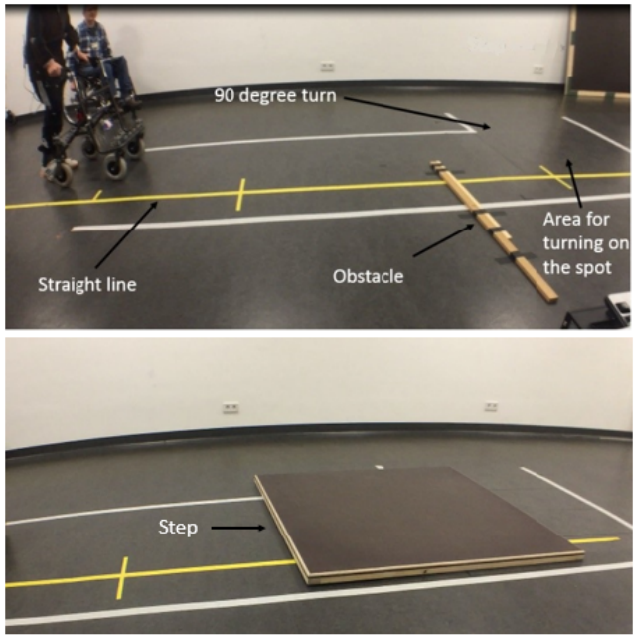

FIGURE 2. Experimental setup in the gait lab, showing the obstacles to be negotiated.

and negotiating a 50mm step up. Each participant was asked to repeat each of the activities twice.

Although all participants started with straight line walking, the order in which the other tasks were performed was varied to avoid learning effects and fatigue related issues.

D. SPEED AND DISTANCE ESTIMATION ALGORITHM

Data from the study were used to develop a two-stage analysis technique to enable speed and distance estimation.

TABLE 1. Activity classification classes and activity types.

Class	Activity Types
Movement	Straight
Turning	Left-Turn, Spot-Turn
Other	Forwards-Backwards, Step, Obstacle

The first stage is activity classification that separates the rollator data into one of three classes (movement, turning or other), subsequently, the speed and distance estimation stage estimates the speed of movement and distance travelled. A separate estimation model is used for each of the three classes of activity to enable more accurate estimation of speed and distance.

1) ACTIVITY CLASSIFICATION

a: ACTIVITY CLASSES

The activity classifier uses a one-vs-one multiclass support vector machine (SVM) [15] to classify each trial into one of six activity types, which are then aggregated into one of three overall categories (termed 'classes'). The three classes used are given in Table 1.

SVMs are well used techniques for classification tasks, especially when there is a large number of features as we have in this study, and operate principally on binary problems. A multi-stage SVMs, which have a track record of use for physical activity classification [16]0–[18], combine several binary SVMs with a voting mechanism to achieve multi-class classification. Furthermore, SVM is a well-known algorithm that works successfully in binary classification scenarios. In the work presented in this paper, a one-vs-one methodology was used where an SVM is trained to recognise one activity type against the remainder, resulting in this case in six individual SVMs being used. The class with the most votes from the one-vs-one classifications is then assigned the class label.

b: FEATURE DESIGN AND SELECTION

Features are calculated from each trial from the following 7 parameters: X, Y, Z and RMS (Root Mean Square) signals from the accelerometer and the X, Y and Z axis signals from the gyroscope. A 43-feature set was (Table 2) used as a base set and additionally, each signal was processed with one of 10 different initial processing techniques (Table 3) before the base set of features was calculated for the signal.

In summary, 3,010 signal features were calculated. Feature selection using Latent Feature Selection [19] (with the FSLib library [20]) was used to reduce this to a more manageable number. A candidate feature set (CFS) was calculated to identify each class against all the others, and the features that occur in all six CFSs were used as the final feature set. Feature selection in this way reduced the feature set to 2,588 features. The SVM classifier was subsequently

TABLE 2. The 43-feature base feature set.

N.	Processing	N.	Processing
1	Max	2	Min
3	Mean	4	Median
5	Sum	6	Standard deviation
7	Variance	8	Mean minus standard deviation
9	Mean plus standard deviation	10	Skewness
11	Kurtosis	12	Mean normalised angular frequency
13	Median normalised angular frequency	14	Peak to peak distance (range)
15	Peak to RMS distance	16	Root mean squared value
17	Root sum squared value	18-27	Frequencies of 10 most dominant frequency components
28	Average power	29	Two-sided equivalent noise bandwidth
30	99% occupied bandwidth	31	3 dB (half power) bandwidth
32	Number of peaks greater than the mean	33	Number of peaks greater than the mean plus one SD
34	Number of peaks greater than the mean plus two SD	35	Number of peaks less than the mean
36	Number of peaks less than the mean minus one SD	37	Number of peaks less than the mean minus two SD
38	Percentage of the signal that is above or below the mean plus one SD	39	Percentage of the signal that is above or below the mean plus two SD
40	Percentage of the signal that is within one SD of the mean	41	Sum of the signal that is above or below the mean plus one SD
42	Sum of the signal that is above or below the mean plus two SD	43	Sum of the signal that is within one SD of the mean

trained with the reduced feature set using the Matlab 2016b Statistics and Machine Learning Toolbox. The SVM classifier was trained and tested using 1000 runs of 10-fold cross-validation, which provide a sensible statistical average in an acceptable runtime.

2) SPEED AND DISTANCE ESTIMATION

The estimator stage is an evolution of previous work by the authors [14], which has been expanded significantly and proceeds in the following manner.

TABLE 3. The 10 pre-processing methods for feature extraction.

N.	Processing	N.	Processing
1	X (raw signal)	2	X-mean(X)
3	Abs(X)	4	Abs(X-mean(X))
5	Smooth(X)	6	Smooth(X-mean(X))
7	Smooth(abs(X))	8	Smooth(abs(X-mean(X)))
9	upperEnvelope(X)	10	lowerEnvelope(X)

a: STATIC ALIGNMENT CORRECTION

The IMU is mounted onto the rollator such that there is a constant static pitch error of around 16 degrees. For the sake of completeness static roll offset is also corrected for at this point. This is corrected through calculation and use of a rotation matrix to adjust the accelerometer and gyroscope data to be aligned with true vertical. Initially, the accelerometer data, $\boldsymbol{A}$, are padded with random noise to match the amplitude of the initial part of the signal and a low pass filter at 0.02 Hz is applied to extract the baseline data. The padding is subsequently removed from the filtered signal to give $\boldsymbol{A}^L = \{A^{Lx}, A^{Ly}, A^{Lz}\}$.

It is assumed that acceleration data is of the form $A^x = \{a_1^x a_2^x, \ldots, a_n^x\}$ and that gyroscope data are of the form $G^x = \{g_1^x g_2^x, \ldots, g_n^x\}$, where the superscript letter indicates the axis, X, Y or Z. The set of all accelerometer data will be denoted as $\boldsymbol{A} = \{A^x, A^y, A^z\}$ and the set of all gyroscope data as $G = \{G^x, G^y, G^z\}$. A single frame of $\boldsymbol{A}$ can be represented as $\boldsymbol{A}_i = \{a_i^x, a_i^y, a_i^z\}$, and similarly for $\boldsymbol{G}$.

Orientation is corrected for by calculating the pitch and roll (α and β) of the IMU over the first 200 samples (two seconds) of the recording, when the rollator is assumed to be static, as:

$$\alpha = \frac{1}{200}\sum_{i=1}^{200} atan\left(\frac{a_i^{Ly}}{\sqrt{a_i^{Lx^2} + a_i^{Lz^2}}}\right) \tag{1}$$

$$\beta = \frac{1}{200}\sum_{i=1}^{200} atan\left(\frac{a_i^{Lx}}{\sqrt{a_i^{Ly^2} + a_i^{Lz^2}}}\right) \tag{2}$$

The rotation matrix R is then constructed as:

$$R_\alpha = \begin{bmatrix} \cos(\alpha) & 0 & -\sin(\alpha) \\ 0 & 1 & 0 \\ \sin(\alpha) & 0 & \cos(\alpha) \end{bmatrix}, \tag{3}$$

$$R_\beta = \begin{bmatrix} 1 & 0 & 0 \\ 0 & \cos(\beta) & -\sin(\beta) \\ 0 & \sin(\beta) & \cos(\beta) \end{bmatrix}, \tag{4}$$

$$R_\gamma = \begin{bmatrix} 1 & 0 & 0 \\ 0 & 1 & 0 \\ 0 & 0 & 1 \end{bmatrix}, \tag{5}$$

$$R = R_\gamma R_\alpha R_\beta, \tag{6}$$

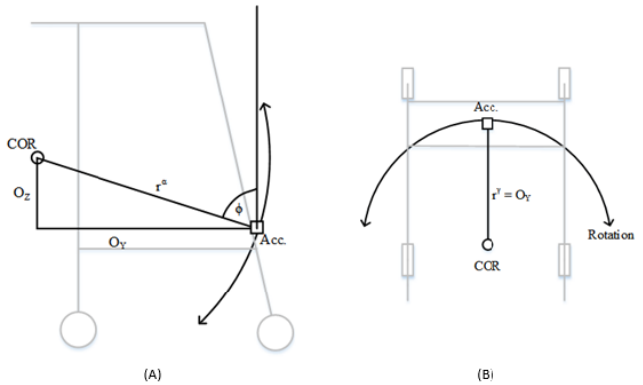

FIGURE 3. Position and abstraction of the offset accelerometer in the plane parallel to the normal direction of travel for correction due to pitch (A) and the horizontal plane for correction due to yaw (B) showing the Accelerometer (Acc.), the centre of rotation (COR), directions of rotation, positioning offsets (O_Y and O_Z), distance to COR (r^α and r^γ), and offset of the accelerometer in relation to the line $r^\alpha(\varphi)$.

And then used to rotate $\boldsymbol{A}$ and $\boldsymbol{G}$ to correct for the static alignment of the IMU, giving $\boldsymbol{A}^R$ and $\boldsymbol{G}^R$ respectively, such that:

$$\boldsymbol{A}_i^R = R \begin{bmatrix} a_i^x \\ a_i^y \\ a_i^z \end{bmatrix}, \quad \forall 1 \leq i \leq n \tag{6a}$$

$$\boldsymbol{G}_i^R = R \begin{bmatrix} g_i^x \\ g_i^y \\ g_i^z \end{bmatrix}, \quad \forall 1 \leq i \leq n \tag{6b}$$

b: FILTERING

Once static alignment has been corrected, both the accelerometer and gyroscope data are filtered with low-pass filters to provide filtered versions of the data that are used further down the processing chain. $\boldsymbol{A}^R$ is filtered (to give $\boldsymbol{A}^{RL}$) using a low-pass Butterworth filter, which is designed on-the-fly as the passband and stopband parameters are optimised in the training step. $\boldsymbol{G}^R$ is filtered, using a 4-section lowpass IIR filter with a cutoff of 6 Hz, to remove high frequency noise, giving $\boldsymbol{G}^{RL}$.

c: OFFSET CENTRE OF ROTATION CORRECTION

Due to the mounting position of the accelerometer on the rollator, shown in Fig. 3 any turning forces applied to the rollator by the user will induce tangential and radial acceleration in the accelerometer that would not be present if the accelerometer were mounted at the centre of rotation (COR). These induced accelerations would introduce errors in the estimation of linear velocity and hence distance travelled if not removed. In this step we use equations of circular motion and an estimate of the COR to estimate the induced acceleration and remove it from the data. The offsets of the COR (r^α and r^γ) from the IMU are optimisation parameters.

The following formula are used to calculate the correction for a particular time point and angular velocity is given by:

$$\omega = \frac{\delta\theta}{\delta t}. \tag{7}$$

Tangential velocity given by:

$$v_t = \omega r \tag{8}$$

and used to calculate tangential velocity components for pitch and yaw,

$$v_t^\alpha = \omega^\alpha r^\alpha, \tag{9}$$
$$v_t^\gamma = \omega^\gamma r^\gamma, \tag{10}$$

where the values for ω are taken from the gyroscope data. Radial acceleration is given by:

$$a_r = \omega^2 r \tag{11}$$

and used to calculate radial acceleration for pitch and yaw components as:

$$a_r^\alpha = \omega^{\alpha^2} r^\alpha, \tag{12}$$
$$a_r^\gamma = \omega^{\gamma^2} r^\gamma. \tag{13}$$

Tangential acceleration for pitch and yaw are calculated as:

$$a_t^\alpha = \Delta v_t^\alpha \times fs, \tag{14}$$
$$0a_t^\gamma = \Delta v_t^\gamma \times fs, \tag{15}$$

where fs is the sample rate in Hz, Δv the change in velocity between one sample and the next.

The angle ϕ is the angle between the line from the COR to the accelerometer and the vertical axis as shown in Figure 3 (A) and is used to determine the fraction of radial and tangential acceleration that manifests in the accelerometer due to fact that the accelerometer is not aligned with the radial or tangential axes if there is a horizontal offset. The angle ϕ is calculated as:

$$\phi = atan\left(\frac{O_Y}{O_Z}\right) \tag{16}$$

and used to calculate the components of radial acceleration and tangential acceleration that project onto the Z and Y axis of the accelerometer.

$$a_t^{\alpha y} = a_t^\alpha cos\,(\phi)\,, \tag{17}$$
$$a_t^{\alpha z} = a_t^\alpha sin\,(\phi)\,, \tag{18}$$
$$a_r^{\alpha y} = a_r^\alpha sin\,(\phi)\,, \tag{19}$$
$$a_r^{\alpha z} = a_r^\alpha cos\,(\phi)\,. \tag{20}$$

The final adjustments to the accelerometer X, Y and Z axis are given by:

$$x = x - a_t^\gamma, \tag{21}$$
$$y = y + a_r^{\alpha y} + a_r^\gamma + a_t^{\alpha y}, \tag{22}$$
$$z = z - a_r^{\alpha z} + a_t^{\alpha z} \tag{23}$$

These corrections are applied at each time-point to the accelerometer data $\boldsymbol{A}^{RL}$ to give $\boldsymbol{A}^C$.

d: CORRECTION OF DYNAMIC PITCH AND ROLL

Dynamic pitch and roll, that is to say, the pitch and roll of the rollator while it is being used, serve to alter the orientation of the device with respect to the earth and cause the forward acceleration to register slightly on axis other than Y. This is corrected in this step to ensure that all forward motion is mapped to the Y axis and all lateral motion mapped to the X axis. Dynamic pitch and roll correction uses the same approach as static pitch and roll correction but replaces the calculation of α and β in Equations (1) and (2) with a complementary filter to calculate the pitch and roll angles at all time points.

$$\alpha_i = 0.98\left(\alpha_{i-1} + \frac{g_i^{RLx}}{100}\right) + 0.02\left(\operatorname{atan}\left(\frac{a_i^{Cy}}{\sqrt{a_i^{Cx^2} + a_i^{Cz^2}}}\right)\right) \tag{24}$$

$$\beta_i = 0.98\left(\beta_{i-1} + \frac{g_i^{RLy}}{100}\right) + 0.02\left(\operatorname{atan}\left(\frac{a_i^{Cx}}{\sqrt{a_i^{Cy^2} + a_i^{Cz^2}}}\right)\right) \tag{25}$$

where

$$\alpha_0 = \operatorname{atan}\left(\frac{a_1^{Cy}}{\sqrt{a_1^{Cx^2} + a_1^{Cz^2}}}\right) \tag{26}$$

$$\beta_0 = \operatorname{atan}\left(\frac{a_1^{Cx}}{\sqrt{a_1^{Cy^2} + a_1^{Cz^2}}}\right) \tag{27}$$

From this point, the rotation matrix is constructed and used in the same way as for static pitch and roll correction for the accelerometer only to give $\boldsymbol{A}^D$.

e: SPEED AND DISTANCE CALCULATION

An initial velocity estimate $\boldsymbol{V}^E$ is calculated using cumulative trapezoidal integration over the X and Y components of $\boldsymbol{A}^D$, such that:

$$v_0^{Ex} = 0, \tag{28}$$

$$v_0^{Ey} = 0, \tag{29}$$

$$v_i^{Ex} = v_{i-1}^{Ex} + \frac{a_{i-1}^{Dx} + a_i^{Dx}}{2}, \tag{30}$$

$$v_i^{Ey} = v_{i-1}^{Ey} + \frac{a_{i-1}^{Dy} + a_i^{Dy}}{2}. \tag{31}$$

Due to the nature of the preceding calculations, and the propensity for accelerometer data to drift, the velocity estimate must be rebased, in accordance with the authors previous work [14]. This is achieved by estimating the baseline by interpolating through the points when the velocity estimate is considered to show no movement, referred to as zero points.

The zero points are identified by finding runs of points where the difference between the upper and lower envelope of the smoothed RMS of the velocity signal is less than a threshold value. The threshold value and minimum run length are optimisation parameters. Once the zero points have been identified, linear interpolation is used to interpolate between the velocities at these points to estimate the baseline, which is then subtracted from the velocity signal. The adjusted velocity signal can then be cumulatively integrated to get distance travelled over time. This is repeated in the X and Y axis and the Euclidian combination of the two gives total distance.

f: TRAINING AND CROSS-VALIDATION

The speed and distance estimator trains up three different estimators, designed to match the three grouped activity categories identified by the 3-class classification. A separate set of three estimators is optimised for each user, with the target of obtaining the same speed as the Vicon data shows. Due to the highly limited quantity of data available, it was not possible to train and test the estimators on separate sets of data. Instead, the estimators in this work show what is possible given the data.

E. DATA PROCESSING

Data were taken from the Vicon data files and the Xsens data files, which had been aligned to synchronise the timestamps of both datasets, and subjected to some pre-processing steps prior to further processing. Initially, Vicon data were downsampled to 100 Hz to match the Xsens data. Secondly, the axis registration of the Xsens data were corrected as some of the trials had the Xsens unit attached incorrectly and rotated through 180 degrees around the Z-axis; the full axis registration from IMU to biological axis is given in Figure 1(C). Finally, the gyroscope data were zeroed by subtracting the mean of the first 200 samples from each signal.

Data files for each recording typically contain two repetitions of each trial. It is worth noting that each of the trials used to train the ''turning'' and ''other'' classifier typically contained data immediately preceding and immediately following the negotiation of the activity in question. For example, ''obstacle'' trials contained data not only of the period during which the rollator was moving over the obstacle, but also some straight walking immediately prior to, and following this. For use in the activity classification stage, these recordings were split in half in the middle of the largest section where there was no Vicon data, giving two trials per recording. Due to the methodology used in the estimator stage this split was not possible so recordings were left containing two trials.

III. RESULTS

A. ACTIVITY CLASSIFICATION

Tables 4 to 7 show the results of the activity classifier applied to the data. The confusion matrix for the full six-class classifier is shown in Table 4 and the derived accuracy measures are shown in Table 5. In all cases, Fwd-Bwd refers to the forward-backwards walk (2.5 m) as if to open a door. The confusion matrix and derived accuracy measures for the reduced three-class classifier are shown in Tables 6 and 7.

TABLE 4. Confusion matrix for the full 6-class one-vs-one SVM classifier showing the mean and standard deviation results over 1000 runs.

		Predicted					
		Straight	Left Turn	Spot Turn	FwdBwd	Step	Obstacle
Actual	Straight	14.65 (±0.57)	0.00 (±0.05)	0.44 (±0.50)	0.91 (±0.29)	0.00 (±0.00)	0.00 (±0.00)
	Left Turn	0.00 (±0.00)	12.31 (±0.90)	3.58 (±0.85)	0.11 (±0.31)	0.00 (±0.00)	0.00 (±0.00)
	Spot Turn	1.00 (±0.00)	4.64 (±0.83)	7.36 (±0.88)	1.01 (±0.31)	0.00 (±0.00)	0.00 (±0.00)
	FwdBwd	1.05 (±0.29)	0.02 (±0.13)	1.01 (±0.07)	9.93 (±0.34)	0.00 (±0.00)	0.01 (±0.07)
	Step	0.00 (±0.00)	0.00 (±0.00)	0.00 (±0.00)	0.00 (±0.03)	10.24 (±0.46)	3.76 (±0.46)
	Obstacle	1.00 (±0.03)	0.00 (±0.00)	0.00 (±0.00)	1.27 (±0.48)	3.69 (±0.57)	8.04 (±0.34)

TABLE 5. Precision, recall and F1 statistics calculated from the average confusion matrix for the 6-class classifier (Table 4).

Task	Precision	Recall	F1
Straight	0.828	0.915	0.869
Left Turn	0.726	0.770	0.747
Spot Turn	0.594	0.525	0.558
FwdBwd	0.751	0.827	0.787
Step	0.735	0.731	0.733
Obstacle	0.681	0.574	0.623
Average	0.719	0.724	0.720

TABLE 6. Confusion matrix for the grouped 3-class problem, generated by aggregating results from Table 4.

		Predicted		
		Straight	Turning	Other
Actual	Straight	14.65 (± 0.57)	0.44 (± 0.55)	0.91 (± 0.29)
	Turning	1.00 (± 0.00)	27.89 (± 3.45)	1.11 (± 0.61)
	Other	2.05 (± 0.32)	1.02 (± 0.20)	36.93 (± 2.75)

B. SPEED AND DISTANCE ESTIMATES

Tables 8 to 11 show results from speed and distance estimates using groupings for training and testing as in the grouped 3-class problem. Figure 4 show example plots for speed and distance traveled: 'Ground truth' data collected using the Vicon measurement system and 'estimated' using the approach presented in this paper.

TABLE 7. Precision, recall and F1 statistics calculated from the average confusion matrix for the 3-class classifier (Table 6).

Task	Precision	Recall	F1
Straight	0.828	0.915	0.869
Turning	0.950	0.930	0.940
Other	0.948	0.923	0.936
Average	**0.909**	**0.923**	**0.915**

TABLE 8. Average absolute error in speed (m/s) over each time point for each trial.

	Task					
P.	Straight	Left Turn	Spot Turn	Fwd-Bwd	Step	Obstacle
1	0.028	0.040	0.100	0.111	0.106	0.101
2	0.025	0.059	0.089	0.196	0.188	0.088
3	0.020	0.063	0.063	0.181	0.144	0.128
4	0.036	0.102	0.122			
5	0.030	0.082	0.121	0.146	0.406	0.063
6	0.051	0.093	0.107	0.178	0.107	0.114
7	0.037	0.058	0.061	0.117	0.116	0.121
8	0.055	0.048	0.062	0.093	0.064	0.082
9	0.081	0.058	0.102	0.179	0.397	0.104
10	0.023	0.090	0.129	0.224	0.152	0.221
Mean	0.039	0.069	0.096	0.143	0.168	0.102
Std	0.018	0.020	0.025	0.062	0.126	0.053

IV. DISCUSSION

This paper has introduced a method to characterize activity types and an improved method for estimating speed and distance travelled with a rollator-mounted IMU sensor. The study involved 10 users of rollators, who walked on a course designed to represent obstacles encountered in daily life, including going up a step and turning a corner. In recognition that IMUs may not always be placed horizontally on a rollator, we also developed a mechanics-based approach to correct for the static offset in orientation of the accelerometer unit with respect to gravity. We also implemented an optimisation approach to compensate for the tangential and radial accelerations seen by the IMU when rotating. Comparisons were made between speed and distance calculated from rollator-mounted IMU sensor data using our algorithm and rollator-mounted reflective marker data.

The classification accuracy of full 6-class, the *straight* task remains fairly high (Precision = 0.828; Recall = 0.915; F1 = 0.869). However the classification results for the

TABLE 9. Percentage error in speed (m/s) over each time point for each trial.

	Task					
P.	Straight	Left Turn	Spot Turn	Fwd-Bwd	Step	Obstacle
1	5.00	16.67	23.75	429.71	237.01	23.02
2	3.73	11.61	25.30	80.63	92.61	119.69
3	3.26	17.50	16.54	74.46	94.19	45.31
4	7.12	20.99	34.59	0.00	0.00	0.00
5	5.04	12.49	19.23	31.13	523.55	9.17
6	10.73	63.95	31.07	76.16	92.93	82.16
7	11.27	17.61	36.16	82.47	243.54	57.83
8	27.60	25.50	55.41	87.19	83.82	82.68
9	11.64	8.12	17.01	62.29	155.82	15.26
10	5.76	25.21	74.19	68.68	386.75	64.87
Mean	9.11	21.97	33.33	99.27	191.02	50.00
Std	6.84	14.97	17.54	113.10	152.21	36.56

TABLE 10. Total error in distance travelled (m) for each trial.

	Task					
P.	Straight	Left Turn	Spot Turn	Fwd-Bwd	Step	Obstacle
1	-0.47	-1.23	-3.12	0.13	-4.61	-5.95
2	-0.43	0.13	0.06	-17.20	-7.73	13.70
3	0.44	-0.15	-1.79	-14.78	-4.14	-5.45
4	-1.20	-3.32	-0.44			
5	0.08	0.70	-2.15	0.05	14.88	-0.40
6	0.54	-2.52	-3.16	-14.83	-7.58	-4.60
7	0.52	0.72	-2.17	-8.93	-6.42	-6.08
8	1.36	-2.84	-2.84	-7.17	-3.28	-8.61
9	2.35	0.80	-1.93	-5.03	11.43	-2.92
10	-0.08	-1.30	-0.61	-10.49	-0.32	-5.57
Mean	0.31	-0.90	-1.82	-7.83	-0.78	-2.59
Std	0.95	1.49	1.08	6.23	7.44	5.98

TABLE 11. Percentage error in distance travelled for each trial.

	Task					
P.	Straight	Left Turn	Spot Turn	Fwd-Bwd	Step	Obstacle
1	-5.01	-13.49	-41.34	0.86	-41.71	-56.60
2	-4.58	1.08	0.39	-98.53	-67.18	128.61
3	4.68	-1.03	-12.15	-99.98	-39.71	-54.06
4	-12.79	-34.90	-2.89	0.00	0.00	0.00
5	0.83	7.49	-14.07	0.34	150.84	-2.34
6	5.81	-26.97	-22.09	-99.92	-74.66	-40.96
7	5.48	7.72	-15.96	-99.81	-63.13	-62.91
8	14.60	-30.56	-38.00	-98.80	-65.61	-85.41
9	25.34	8.97	-13.11	-36.76	114.97	-31.98
10	-1.87	-13.04	-4.07	-82.14	-7.11	-69.89
Mean	3.25	-9.47	-16.33	-61.47	-9.33	-27.55
Std	10.24	15.91	13.31	44.41	75.39	58.24

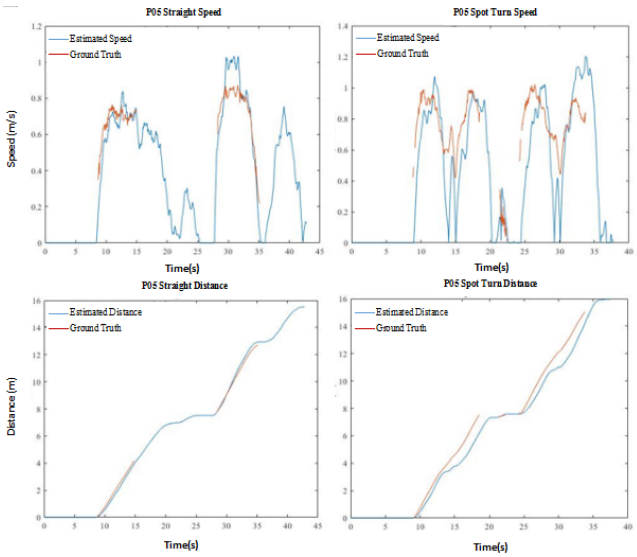

FIGURE 4. Example data (participant 05) for estimated and marker-derived speed and distance. Top left: "Straight Speed"; Top right: "Spot Turn Speed"; Bottom left: "Straight distance"; Bottom right: "Spot Turn distance". Please note that the participants sometimes moved outside of the Vicon camera capture volume and these periods correspond to the gaps in the ground truth data.

remaining tasks are somewhat mixed. In particular, there is a large amount of cross-class confusion between *Left Turn* and *Spot Turn* and between *Step* and *Obstacle*. This is perhaps unsurprising, given the similarities between, for example, obstacle and step crossing and being able to discriminate between the two may be of limited relevance to clinicians. Therefore, we also investigated the performance of a classifier which considered only 3 classes (straight, turning and other). The classification accuracy improved, with precision, accuracy and F1 statistics all greater than 0.9.

Overall, the performance of our estimation on speed was satisfied. The mean absolute errors for the straight, left turn

and spot turn were below 0.1 m/s, which is a limit of clinically meaningful differences in walking speed [21]. The step task was the worst case with a mean absolute error of 0.2 m/s, although the clinical relevance of this error has yet to be determined. To allow comparison, various approaches to estimating gait speed from body worn IMUs have been reported. Results vary with both body location and methods used. For example, Laudanski and colleagues [22] showed RMSE of 0.14 m/s from a shank-mounted IMU; an approach based on a wrist worn IMU resulted in accuracy and precision of 5.9% and 4.7%, respectively [23]. It is worth noting that many previous studies have used healthy young subjects, whose walking was likely to be more regular than the participants in this study.

Very small absolute percentage error (mean percentage error = 5.16%) of the straight task was achieved for distance travelled estimation. It is clear, the distance travelled estimation for the remaining tasks were very poor. The mean errors are ranging from 18.02% - 72.31%. It is worth noting that the absolute distance travelled during some of these activities was rather small and hence may have limited effect on the perhaps more clinically important measure of total distance travelled.

It is worthwhile to compare the findings in this paper with our previous research [14]. In our earlier work we collected data over a number of periods of straight line walking over different surfaces. In addition, one of the two subjects studied was unimpaired. In both subjects, the pushing style was characterized by push events, each fairly consistently separated by periods of no movement. The data was relatively straightforward to analyse and showed promise in terms of prediction of both walking speed and distance travelled. However, it is clear from this study that the pushing style seen in our earlier study may not have been representative of a wider population. Of our 10 participants, by contrast to our previous study [14], none showed a clear pattern of distinct push events interspersed with low velocity periods (See last Figure). This observation is consistent with a previous study [24].

There are clear practical advantages to mounting sensors on walking aids, as opposed to the person themselves, particularly when studying behaviors over extended periods of time. For example, the tolerance for wearable sensors is limited and participants periodically remove sensors, for example when sleeping, requiring algorithms to distinguish periods of wear from non-wear. Nevertheless, monitoring based solely on a sensor on the walking aid provides no direct observation of the user themselves and therefore provides no data on periods of unassisted mobility. Further, there is the potential to misattribute observations from a rollator-mounted sensor to the wrong individual, particularly in settings such as care homes where multiple users of rollators may be in the same building. Further work is needed in the future to better understand when a single sensor on the rollator provides sufficient information and when multiple sensors may be required.

By contrast to the extensive work interpreting data from body-worn sensors [25], methods to interpret sensor data from walking aids is in its infancy. For example, Culmer and colleagues investigated the potential for an instrumented walking stick (sometimes referred to as a 'cane') to be used for gait assessment and training [26]. A recent paper has shown the potential to estimate distance travelled from walking stick-mounted IMU [27]. In other related work, three of the authors (EM, ST and LK) have shown the potential for characterizing stability through a combination of instrumented walking aids, insole pressure systems and an optoelectronic position tracking system [28]. Longer term we see the potential to extend and combine some of these techniques to better understand both mobility and fall events in vulnerable older adults.

One of the limitations of this work is the relatively limited number of participants (all of whom were trained at the same centre in Germany) and the low number of repetitions of each activity by each participant. This forced an approach to the machine learning which could lead to over specialising of the resultant classifiers and estimators. This was unavoidable given the data that were available and the results presented here showcase the best possible outcome. Further work in this area would need to include more participants and more repetitions of each activity in order to build a robust classifier.

V. CONCLUSION AND FUTURE WORK

The study has shown the potential to use a machine learning approach to estimate rollator velocity and distance travelled from a single IMU located on a four wheeled rollator. The results show promise, but further work with a larger data set and an increased number of subjects is needed to confirm the performance of our approach. While the decision to use a SVM as the classifier in this work is supported by the promising results, it would be interesting to compare the performance with other classifiers in future work. Our methods show promise as a tool to better understand older people's use of mobility aids in the urban environment.

REFERENCES

[1] L. I. Iezzoni, E. P. McCarthy, R. B. Davis, and H. Siebens, "Mobility difficulties are not only a problem of old age," *J. Gen. Internal Med.*, vol. 16, no. 4, pp. 235–243, Apr. 2001.

[2] *Disability in the United Kingdom 2016 Facts and Figures*. Papworth Everard, U.K.: Papworth Trust, 2016.

[3] C. Löfqvist, C. Nygren, Z. Széman, and S. Iwarsson, "Assistive devices among very old people in five European countries," *Scand. J. Occupational Therapy*, vol. 12, no. 4, pp. 181–192, 2005.

[4] H. S. Kaye, T. Kang, and M. P. LaPlante, "Mobility device use in the United States: Disability statistics report," U.S. Dept. Educ., Nat. Inst. Disab. Rehabil. Res., Washington, DC, USA, Tech. Rep. 14, 2000.

[5] Å. Brandt, S. Iwarsson, and A. Ståhl, "Satisfaction with rollators among community-living users: A follow-up study," *Disab. Rehabil.*, vol. 25, no. 7, pp. 343–353, 2003.

[6] K. Samuelsson and E. Wressle, "User satisfaction with mobility assistive devices: An important element in the rehabilitation process," *Disab. Rehabil.*, vol. 30, no. 7, pp. 551–558, 2008.

[7] L. Böcker, P. van Amen, and M. Helbich, "Elderly travel frequencies and transport mode choices in greater Rotterdam, The Netherlands," *Transportation*, vol. 44, no. 4, pp. 831–852, Jul. 2017.
[8] W. Liu, H. Lu, Z. Sun, and J. Liu, "Elderly's travel patterns and trends: The empirical analysis of Beijing," *Sustainability*, vol. 9, no. 6, p. 981, 2017.
[9] U. Lindemann, M. Schwenk, J. Klenk, M. Kessler, M. Weyrich, F. Kurz, and C. Becker, "Problems of older persons using a wheeled walker," *Aging Clin. Exp. Res.*, vol. 28, no. 2, pp. 215–220, 2016.
[10] U. Lindemann, M. Schwenk, S. Schmitt, M. Weyrich, W. Schlicht, and C. Becker, "Effect of uphill and downhill walking on walking performance in geriatric patients using a wheeled walker," *Zeitschrift für Gerontologie und Geriatrie*, vol. 50, no. 6, pp. 483–487, 2017.
[11] N. M. Salbach, K. K. O'Brien, D. Brooks, E. Irvin, R. Martino, P. Takhar, S. Chan, and J.-A. Howe, "Reference values for standardized tests of walking speed and distance: A systematic review," *Gait Posture*, vol. 41, no. 2, pp. 341–360, Feb. 2015.
[12] S. S. Kuys, N. M. Peel, K. Klein, A. Slater, and R. E. Hubbard, "Gait speed in ambulant older people in long term care: A systematic review and meta-analysis," *J. Amer. Med. Directors Assoc.*, vol. 15, no. 3, pp. 194–200, 2014.
[13] M. Sanjak, V. Langford, S. Holsten, N. Rozario, C. G. M. Patterson, E. Bravver, W. L. Bockenek, and B. R. Brooks, "Six-minute walk test as a measure of walking capacity in ambulatory individuals with amyotrophic lateral sclerosis," *Arch. Phys. Med. Rehabil.*, vol. 98, no. 11, pp. 2301–2307, Nov. 2017.
[14] T.-J. Cheng, L. Kenney, J. D. Amor, S. B. Thies, E. Costamagna, C. James, and C. Holloway, "Characterisation of rollator use using inertial sensors," *Healthcare Technol. Lett.*, vol. 3, no. 4, pp. 303–309, Dec. 2016.
[15] J. Weston and C. Watkins, "Multi-class support vector machines," Dept. Comput. Sci., Royal Holloway, Univ. London, London, U.K., Tech. Rep. CSD-TR-98-04, 1998.
[16] D. Anguita, A. Ghio, L. Oneto, X. Parra, and J. L. Reyes-Ortiz, "Human activity recognition on smartphones using a multiclass hardware-friendly support vector machine," in *Proc. Int. Workshop Ambient Assist. Living*, Vitoria-Gasteiz, Spain, Dec. 2012, pp. 216–223.
[17] A. Mannini and A. M. Sabatini, "Machine learning methods for classifying human physical activity from on-body accelerometers," *Sensors*, vol. 10, no. 2, pp. 1154–1175, 2010.
[18] F. Attal, S. Mohammed, M. Dedabrishvili, F. Chamroukhi, L. Oukhellou, and Y. Amirat, "Physical human activity recognition using wearable sensors," *Sensors*, vol. 15, no. 12, pp. 31314–31338, 2015.
[19] G. Roffo, S. Melzi, U. Castellani, and A. Vinciarelli, "Infinite latent feature selection: A probabilistic latent graph-based ranking approach," in *Proc. IEEE Int. Conf. Comput. Vis.*, Venice, Italy, Oct. 2017, pp. 1398–1406.
[20] G. Roffo. (2018). *Feature Selection Library*. [Online]. Available: https://uk.mathworks.com/matlabcentral/fileexchange/56937-feature-selection-library
[21] S. Perera, S. H. M. PharmD, R. C. Woodman, and S. A. Studenski, "Meaningful change and responsiveness in common physical performance measures in older adults," *J. Amer. Geriatrics Soc.*, vol. 54, no. 5, pp. 743–749, May 2006.
[22] A. Laudanski, S. Yang, and Q. Li, "A concurrent comparison of inertia sensor-based walking speed estimation methods," presented at the IEEE Annu. Int. Conf. Eng. Med. Biol. Soc., 2011.
[23] S. Zihajehzadeh and E. J. Park, "Regression model-based walking speed estimation using wrist-worn inertial sensor," *PLoS One*, vol. 11, no. 10, Oct. 2016, Art. no. e0165211.
[24] J. Y. Tung, "Development and evaluation of the iWalker: An instrumented rolling walker to assess balance and mobility in everyday activities," Ph.D. dissertation, Graduate Dept. Rehabil. Sci., Univ. Toronto, Toronto, ON, Canada, 2010.
[25] F. Horak, L. King, and M. Mancini, "Role of body-worn movement monitor technology for balance and gait rehabilitation," *Phys. Therapy*, vol. 95, no. 3, pp. 461–470, Mar. 2015.
[26] P. R. Culmer, P. C. Brooks, D. N. Strauss, D. H. Ross, M. N. Levesley, R. J. O'Connor, and B. B. Bhakta, "An instrumented walking aid to assess and retrain gait," *IEEE/ASME Trans. Mechatronics*, vol. 19, no. 1, pp. 141–148, Feb. 2014.
[27] D. C. Dang and Y. S. Suh, "Walking distance estimation using walking canes with inertial sensors," *Sensors*, vol. 18, no. 1, p. 230, 2018.
[28] E. Costamagna, S. B. Thies, L. P. J. Kenney, D. Howard, A. Liu, and D. Ogden, "A generalisable methodology for stability assessment of walking aid users," *Med. Eng. Phys.*, vol. 47, pp. 167–175, Sep. 2017.

MINGXU SUN was born in Jinan, China, in 1984. He received the B.S. degree in control engineering from the University of Jinan, in 2007, and the M.S. degree in manufacturing engineering and the Ph.D. degree in medical engineering from the University of Salford, Manchester, U.K., in 2014.

Following periods of Postdoctoral work with the Rehabilitation Technologies and Biomedical Engineering Group at University of Salford, he was appointed as an Assistant Professor in rehabilitation technologies with the School of Electrical Engineering, University of Jinan, in 2018. His research interests includes the development of functional electrical stimulation systems for use in stroke rehabilitation, together with novel approaches of using inertial sensors for their control; the use of inertial sensors to understand the real world use of walking aids.

JAMES AMOR is a Biomedical Engineer with the University of Warwick. His research interest includes the development of computationally intelligent techniques to extract meaning from multi-sensor systems for applications in health and wellbeing and the use of wearable technology as a data gathering platform within these systems. His work primarily involves the application of intelligent data analysis techniques to large, personal data-sets to extract personalised behaviour patterns, and detect differences in behaviour, which are indicative of changing health state. His work also involves the use of wrist-worn wearable devices, particularly smart-watches and accelerometers to monitor location and activity in a longitudinal setting, and the development of signal processing techniques to detect and analyse activity and movement from these sensors.

CHRISTOPHER J. JAMES (M'92–SM'02) was born in Malta. He received the B.Eng. (Hons.) degree in electrical engineering from the University of Malta, in 1992, and the Ph.D. degree from the University of Canterbury, New Zealand, in 1997, through the Commonwealth Scholarship.

After briefly working in the semiconductor manufacturing with ST Microelectronics, from 1991 to 1993, he was a Postdoctoral Research Fellow of the EEG Department, Montreal Neurological Institute, McGill University, Montreal, Canada, from 1997 to 1998. From 1998 to 2001, he was a Postdoctoral Research Fellow of the Neural Computing Research Group, Aston University, Birmingham, U.K. He was a Lecturer with the Neural Computing Research Group, until 2003. Then, he was a Reader in biomedical signal processing with ISVR, University of Southampton. From 2010 2015, he was a Professor of healthcare technology with the University of Warwick and the Director of the Institute of Digital Healthcare. He is currently a Professor of biomedical engineering and the Director of Warwick Engineering in Biomedicine, University of Warwick. His research interest includes the analysis of EEG and magnetoencephalogram (MEG) signals through intelligent signal and pattern processing techniques, such as artificial neural networks, specifically when applied to epilepsy analysis and for brain-computer interfacing. He is also interested in the development of wearable technology for the assessment of behavior and behavior analysis techniques. Furthermore, he is interested in the development of blind source separation and independent component analysis-based techniques for practical implementation in multi-channel and single channel biomedical signal recordings.

Prof. James is a member of the IEEE Engineering in Medicine and Biology (EMB) Society. He was the past Europe Representative on the EMB Administrative Committee. He was the Chair of the U.K. and Ireland EMBS Chapter, and past IEEE Region Eight Vice Chair for Technical Activities. He is the Founding Editor-in-Chief of *Healthcare Technology Letters* with the IET.

ELEONORA COSTAMAGNA received the bachelor's and master's degrees in biomedical engineering from the Polytechnic University of Turin, Italy, in 2011 and 2014, respectively, and the Ph.D. degree in biomedical engineering from the University of Salford, under the prestigious Pathway to Excellence Studentship Scheme. Prior to starting the Ph.D. degree, in 2015, she was a Graduate Research Trainee for one year with the University of Sydney, where she developed a computational model of stem cells expansion in bioreactors. Her research interests include the safety of walking aids and fall prevention, but her academic interests extend to rehabilitation technologies and assistive devices. In 2014, she has received a scholarship in the field of rehabilitation engineering from the Italian Institute of Technology (IIT).

SIBYLLE THIES received the Ph.D. degree in biomedical engineering and biomechanics from the University of Michigan, USA, in 2004. Her expertise lies in the 3D analysis of human movement using optoelectronic cameras, and inertial and force sensors and processing their signals. She came to the University of Salford, as a Postdoctoral Researcher, in 2005, to work on the European Framework VI Project Healthy AIMS, within which she supported the development of a movement pattern recognition algorithm to trigger functional electrical muscle stimulation in the forearm, to assist stroke survivors with their hand opening. She was with the EPSRC-Funded IDGO TOO Project (inclusive design for getting outdoors), specifically, she led the experimental gait analysis of older people when crossing the road, to investigate the effect of tactile pavement on gait. In 2011, she became a Permanent Staff of the University of Salford. She has worked on a number of projects concerned with gait stability of older adults, with a special focus on walking aid ambulation. She has published over 30 peer-reviewed publications, regularly presented at international and national conferences. She is an active reviewer of a number of journals in her research field.

ULRICH LINDEMANN received the Ph.D. degree, in 2004. He is a Senior Researcher with the Department of Geriatrics and Clinic for Geriatric Rehabilitation, Robert-Bosch-Hospital, Stuttgart. After working as a Professional Coach, from 1989 to 1990, and as a Therapist in orthopaedic and neurologic rehabilitation, from 1990 to 1998, he started as a Research Fellow of the Geriatric Centre Ulm/Alb-Donau, Academic Centre of the University of Ulm, from 1998 to 2004. He wrote the Ph.D. thesis with the University of Ulm. He is involved in teaching of bachelor's and master's degree students (medical school, sport science, and physiotherapy) concerning the subject of strength and balance exercise for older persons, the assessment of physical performance and physical activity, and environmental effects on physical performance and physical activity, representing his research activities.

JOCHEN KLENK received the Diploma degree in medical engineering, the master's degree in public health, and the Ph.D. degree in human biology. He is currently a Professor of public health with the IB University of Applied Sciences, Berlin. He is also a Senior Research Fellow with the Institute of Epidemiology and Medical Biometry, Ulm University, and the Department of Geriatrics and Clinic for Geriatric Rehabilitation, Robert-Bosch-Hospital, Stuttgart. His main research interests include the epidemiology of successful ageing, sensor-based physical activity monitoring, and sensor-based fall measurements.

LAURENCE KENNEY received the B.S. degree in mechanical engineering and the PhD. degree from the University of Salford, in 1993. Following periods of Postdoctoral work in U.K. and The Netherlands, he was appointed to a permanent position with the University of Salford, in 2000. Since 2014, he has been a Professor in rehabilitation technologies with the Centre for Health Sciences Research, University of Salford. His research interests include design and novel approaches to the evaluation of prosthetics, functional stimulation systems, and most recently walking aids. He is a member of the EPSRC Peer Review College, the Chair of the Scientific Committee of the Inspire Charity, and also the Chair of the 2019 Trent International Prosthetics Symposium.